Solar Energy Materials & Solar Cells 94 (2010) 1358–1370

Contents lists available at ScienceDirect

Solar Energy Materials & Solar Cells

journal homepage: www.elsevier.com/locate/solmat

An improved five-parameter model for photovoltaic modules

Valerio Lo Brano *, Aldo Orioli, Giuseppina Ciulla, Alessandra Di Gangi

D.R.E.AM. Dipartimento di Ricerche Energetiche ed AMbientali, Università degli Studi di Palermo, Viale delle Scienze Edificio 9, 90128 Palermo, Italy

ARTICLE INFO

Article history:
Received 10 November 2009
Received in revised form
22 March 2010
Accepted 1 April 2010
Available online 21 April 2010

Keywords:
Photovoltaic modules
Five-parameter model
I–V characteristics
Solar energy
One-diode equivalent circuit
Operating photovoltaic current

ABSTRACT

This paper presents a new five-parameter model capable of analytically describing the *I–V* characteristic of a photovoltaic module for each generic condition of operative temperature and solar irradiance. The parameters of the equivalent electrical circuit are extracted by solving a system of equations based on data commonly issued by manufacturers in standard rating conditions with a trial and error process. The procedure, which does not require any special equations solver, can be easily coded into a short software routine using simple languages and finds the solution of the system of equations with the desired accuracy without needing to be guided towards solutions starting from fitted initial values of the searched parameters.

In particular, as implemented in VBA macros in Microsoft Excel, the model provides the most accurate results with a rapid convergence. To verify the capability of the new model to fit PV panel characteristics, the procedure was tested on two different panels. Results were compared with the data issued by manufacturers and with the results obtained using five-parameter models proposed by other authors.

1. Introduction

Direct conversion of solar radiation into electrical energy avoids the production of pollutants during operation and reduces global warming. The rapid decrease in the photovoltaic (PV) module cost and the escalation in the price of petrochemical fuels have encouraged the diffusion of PV systems that, in the past, were considered attractive only for special applications in remote isolated areas. Due to modern inverters, which can be directly connected to the national grid and are equipped with maximum power point trackers, PV solar electricity has reached technological maturity. Nowadays, PV systems are simple and easy to set up; for this reason, many building owners have become interested in them because they believe they can advantageously exploit the abundant, free, clean and inexhaustible solar energy collected by their roofs. Nevertheless, to encourage the utilization of PV systems, it is essential to allow investors to meet their expectations about the economical feasibility because the investment and utilization costs are still high. Additionally, because of the decline in performance due to long exposure to the sun and bad weather, PV systems also need regular maintenance and device substitution. Because the payback period is usually quite long, it is important to assess accurately the power a PV system can produce in order to correctly estimate the benefit of the economic investment.

The performance of a PV module largely depends on the availability of solar radiation and on the conversion efficiency; these important features are affected by many physical parameters like the site latitude, the typical weather conditions, the panel tilt and azimuth angles, the air temperature, the wind speed, the temperature of the surrounding surfaces, the obstruction and shadow effects, the electrical load, etc. The conversion efficiency mainly depends on the solar irradiation, the silicon slab operating temperature and the electrical load. Because the conversion efficiency can hardly surpass a maximum value of 20%, great attention should be paid to its evaluation. Energy assessments based on the mean constant value of the conversion efficiency can yield erroneously optimistic economical predictions that cannot meet expectations and thus disillusion the trusting investors.

It is well known that predictive performance tools are an important factor in the success of any technology; the ability to optimize the performance of a PV system allows consumers to maximize the cost effectiveness of the system before installing it. In fact, predictive tools can demonstrate whether or not a system will be economically feasible.

PV module manufacturers provide performance data for their products only for fixed standard conditions of solar irradiance and operating temperature. Indeed, sometimes, only a few electrical parameters (maximum power, maximum efficiency) are given. On the contrary, the best manufacturers, who are aware of the importance of good technical information, issue many other interesting data (maximum power voltage and current, short circuit current, open circuit voltage, short circuit current and open

* Corresponding author. Tel.: +390 91 236118; fax: +390 91 484425.
E-mail address: lobrano@dream.unipa.it (V. Lo Brano).

0927-0248/$ - see front matter © 2010 Elsevier B.V. All rights reserved.
doi:10.1016/j.solmat.2010.04.003

Nomenclature

G	solar irradiance (W/m^2)
G_{ref}	solar irradiance at standard rating conditions (1000 W/m^2)
I	current generated by the panel (A)
I_D	diode current (A)
I_L	photocurrent (A)
$I_{L,ref}$	photocurrent at standard rating conditions (A)
I_{mp}	current at the maximum power point (A)
$I_{mp,ref}$	current at the maximum power point at standard rating conditions (A)
I^*_{mp}	current at the maximum power point with $T=T^*$ and $G=G_{ref}$
I_{sc}	short circuit current of the panel (A)
$I_{sc,ref}$	short circuit current of the panel at standard rating conditions (A)
I_0	reverse saturation current (A)
$I_{0,ref}$	reverse saturation current at standard rating conditions (A)
K	thermal correction factor (Ω/°C)
k	Boltzmann constant (1.381×10^{-23} J/K)
n	diode quality factor
P	power generated by the PV panel (W)
q	electron charge (1.602×10^{-19} C)
R_L	electrical load (Ω)
R_s	series resistance (Ω)
R_{so}	reciprocal of slope of the I–V characteristic of the panel for $V=V_{oc}$ and $I=0$ (Ω)
R_{sh}	shunt resistance (Ω)
R_{sho}	reciprocal of the slope of the I–V characteristic of the panel for $V=0$ and $I=I_{sc}$ (Ω)
T	temperature of the PV cell (K)
T_{ref}	temperature of the panel at standard rating conditions (25 °C–298.15 K)
T^*	temperature of the panel different from T_{ref} with $G=G_{ref}$
V	voltage generated by the PV panel (V)
V_{mp}	voltage at the maximum power point (V)
$V_{mp,ref}$	voltage at the maximum power point at standard rating conditions (V)
V^*_{mp}	voltage at the maximum power point with $T=T^*$ and $G=G_{ref}$
V_{oc}	open circuit voltage of the panel (V)
$V_{oc,ref}$	open circuit voltage of the panel at standard rating conditions (V)
α_G	ratio between the current irradiance and the irradiance at standard rating conditions
$\mu_{I,sc}$	thermal coefficient of the short circuit current (A/°C)
$\mu_{V,oc}$	thermal coefficient of the open circuit voltage (V/°C)

circuit voltage temperature coefficients, internal series resistance, curve corrector factor, maximum power current and voltage temperature coefficients, etc.). Moreover, these manufacturers usually give current–voltage (I–V) curves for different fixed values of the irradiance with an operative temperature of 25 °C; they also provide the same curves at different fixed values of the operative temperature with an irradiance of 1000 W/m^2. Even though such data are the result of many painstaking measurement sessions, this information is not valid outwards from the standard conditions. Indeed, the PV panel will always operate far from these standard conditions. For this reason, it is very important to have a reliable model of the PV panel that is able to predict the electrical performance, even though the solar irradiance, the electrical load and the operating temperature do not correspond to the standard conditions.

2. Traditional approach to the problem

The general approach to assess the electrical performance of a PV system is based upon the capability of analytically describing the I–V characteristic of the photovoltaic component for each operative temperature and solar radiation.

Traditionally, the analytical models used in the study of these phenomena evaluate the behaviour of the PV cell by assimilating it into an equivalent electrical circuit that includes some non-linear components. The parameters describing the equivalent electrical circuit are directly related to the performance characteristics of the panel, which are generally available in a graphic form with respect to standard values of temperature and incident radiation.

To better understand the origin of the equivalent circuit, it is useful to remember that a PV cell consists of two layers of semiconductor material, usually silicon, differently doped and electrically connected to two metallic electrodes deposited on their outer surfaces. The upper electrode, which must not obstruct the solar radiation, is deposited with a discontinuous structure embedding several metal elements (fingers), whose shape and size are chosen with the aim of maximizing the absorbing surface and of minimizing finger contact resistance with the silicon.

If it is not illuminated, the cell behaves like a semiconductor junction, a simple diode, whose I–V curve is traditionally described by the equation:

$$I_D = I_0\left(e^{qV/\varepsilon kT}-1\right) \tag{1}$$

where I_0 is the reverse saturation current of the diode, q the electron charge (1.602×10^{-19} °C), k the Boltzmann constant (1.381×10^{-23} J/K), T the junction temperature and ε, which depends on the kind of the semiconductor, varies between 1 and 2.

The illumination of the semiconductor junction generates electron–hole pairs that yield a current I_L, called the photocurrent. An ideal PV cell can be represented by a current source with intensity I_L, connected in parallel with a diode, and the corresponding I–V characteristic is described by the PV cell Shockley [1] equation

$$I = I_L - I_0\left(e^{qV/\varepsilon kT}-1\right) \tag{2}$$

Because the photocurrent I_L is closely related to the photon flux incident on the cell, which is usually independent of the voltage, the characteristic of an ideal PV cell can be obtained from the corresponding characteristic of a diode in the dark by sliding the diode characteristic along the current axis by I_L.

This description is only theoretical because it does not consider the presence of the electrodes, which are necessary to collect the current. In a real diode, the electrodes face each other, and the carriers of electricity flow through the silicon slabs following linear paths, perpendicular to the junction. On the contrary, in a PV cell, due to the discrete shape of the upper electrode, the carriers of electricity follow curved paths toward the fingers that collect them (Fig. 1).

As Wolf [2] observed, in a PV cell, the photocurrent is not generated by only one diode but is the global effect of the presence of a multitude of flanked diodes that are uniformly distributed throughout the surface that separates the two semiconductor slabs. The current through each elementary diode

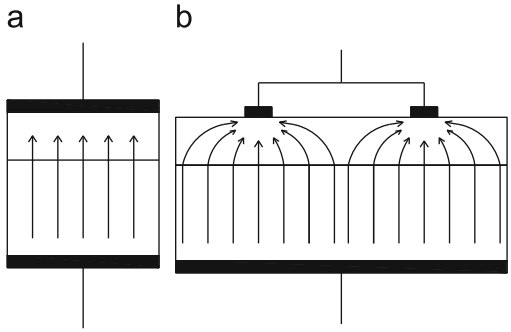

Fig. 1. Schematic electrical charges flow paths in a diode (a) and in a PV cell (b).

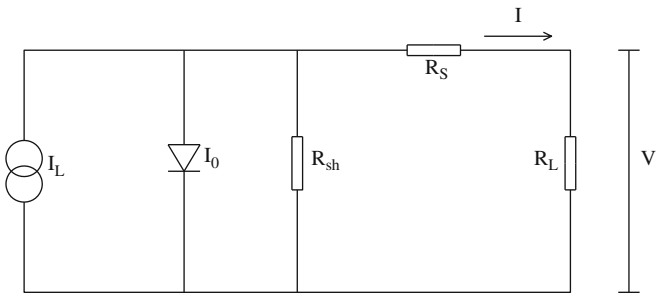

Fig. 2. Equivalent one-diode circuit for a PV panel.

crosses the semiconductor slabs, following different paths that also have different resistances and voltage drops. For each diode, the transversal path component, which is parallel to the cell surface, is different, and thus the *I–V* characteristic for each diode will be different. The combination of such elementary characteristics yields the global *I–V* characteristic of the PV cell. Because the transversal resistances are greater than those related to the straight paths across the semiconductor, they cause high energy consumption and a low conversion efficiency.

To understand the physical behaviour of a PV cell, it is useful to create an electrical equivalent model based on some discrete electrical components. Wolf described the PV cell with an equivalent electric circuit containing a multitude of different lumped elementary components, each one made up of a current generator, a diode and a series resistance. Such an equivalent circuit was too complex to be used, and a simplified equivalent circuit was eventually proposed. The circuit contains only one pair of diodes, a current generator and two resistors, R_s and R_{sh}, which are employed to take into account of the dissipative effects described before and of the presence of any construction defects that can cause parasite currents within the PV panel.

The two-diode model requires the determination of seven parameters that variously affect the shape of the *I–V* characteristic. In particular, the resistances R_{sh} and R_s change the slope of the *I–V* characteristic, before and after the curve "knee", respectively, while the ratio between the reverse saturation currents tends to modify the curvature [3].

Although it is not a problem that is mathematically indeterminate, the calculation of the seven parameters is not easy because of the implicit form of the equation and the presence of two exponential terms. In the literature there are only a few examples concerning the solution of the seven-parameter equivalent circuit. Furthermore, they relate to the single cell and not the entire panel and are limited by specific assumptions [4–6]. The cited methods are very sensitive to the initial conditions and, if not properly guided by an initial estimate of the parameters, lead to inconsistent results. For this reason, some authors preferred to use different types of correlations that are not based on an electrical model [7,8], and others have used a simplified model with a single diode (Fig. 2), which is described by the following five-parameter implicit equation:

$$I = I_L - I_0\left(e^{(V+IR_s)/nT} - 1\right) - \frac{V+IR_s}{R_{sh}} \tag{3}$$

where following the traditional theory, the photocurrent I_L depends on the solar irradiance, the reverse saturation current I_0 is affected by the PV cell temperature, and n, R_s and R_{sh} are constant.

It is important to observe that, for complex phenomena, it is unrealistic to assume that I_0, R_s and R_{sh} are constant. Actually, each elementary diode forming the PV cell should have a different value of I_0, whereas the resistances R_s and R_{sh} do not physically exist, as they only are the electrical representation of the energy losses and voltage drops occurring in the presence of the photocurrent. Moreover, it is also unrealistic to consider that the behaviour of the PV cell, which is also affected by the reverse saturation current thermal drift, can be described using, for each elementary diode, the same correlation of I_0 with the temperature, derived by the theory of semiconductors. In other words, it is necessary to forget that a PV cell is an illuminated diode and to try to change the approach to the problem.

The aim of the present paper is to propose an improved form of the five-parameter model able to accurately represent the electric behaviour of a PV module on the basis of the technical information commonly issued by manufactures. Even though the model is described by an equation quite similar to that used for the traditional five-parameter model, it contains some relevant differences that show the importance of the dependence of I_0, R_s and R_{sh} on the solar irradiance and temperature. This result is achieved with no lack of simplicity and maintains a high accuracy in the evaluation of the panel performance at any value of temperature and irradiance far from the standard conditions.

3. The five-parameter model

Despite the previous considerations, the one-diode model must not be rejected. Actually, it adequately fits with the *I–V* characteristic at standard rating conditions (SRC) – irradiance $G=1000\ \mathrm{W/m^2}$ and cell temperature $T=25\ ^\circ\mathrm{C}$ – of most of the modern and efficient PV modules, which, because they have a small R_s and a large R_{sh}, show a good fill factor and, consequently, an *I–V* characteristic with a very sharp bend. On the contrary, it may be quite impossible to represent slightly curved *I–V* characteristics using only one exponential term. For this reason, other authors have focused on the one-diode model and have recently proposed some interesting improvements that allow the determination of the five parameters on the basis of the performance data typically provided by manufacturers.

De Soto et al. [9] proposed a model for the evaluation of the PV array performance obtained using the values of the short circuit current I_{sc}, the open circuit voltage V_{oc} and the maximum power voltage V_{mp} and current I_{mp} at SRC. A fourth piece of information resulted from the recognition that the derivative of the power at the maximum power point is zero. Eventually, the temperature coefficient of V_{oc} was used to write the fifth relation necessary to find the five parameters. To take into account the dependence of the parameters on the operating temperature, the reverse saturation current was evaluated with a relationship derived by the Townsend equation [10]; whereas, for the photocurrent I_L, the temperature coefficient of the short circuit current was used. The resistances R_s and R_{sh} were considered constant, and I_L was

assumed to be linearly proportional to the solar irradiance. The simultaneous solution of the equations was performed by means of a non-linear equation solver. This method of obtaining the model parameters is usually inadequate because of the difficulties that can be encountered with these powerful mathematical tools.

De Blas et al. [11] used the values of I_{sc}, V_{oc}, V_{mp} and current I_{mp} at SRC to verify the Eq. (3) in correspondence with such I–V points. Moreover, they also evaluated the derivatives of Eq. (3) in the short circuit and open circuit points and made them equal to the reciprocal of slopes of the characteristic curve in these points, called R_{sho} and R_{so}, which can be graphically evaluated from the standard I–V curves issued by manufacturers. These positions permitted to write five equations and the searched parameters were extracted using them with a series of simplifications based on the following analytical positions:

$$e^{I_{sc}R_s/nT} \ll e^{V_{oc}/nT} \quad \frac{I_0}{nT}e^{I_{sc}R_s/nT} \ll \frac{1}{R_{sh}} \tag{4}$$

which are usually widely satisfied. By means of such simplifications, it is possible to write the explicit expressions of the five parameters evaluated by a process of trial and error based on the initial estimate of R_s.

In order to adapt PV model behaviour to different conditions of temperature and irradiance, De Blas et al. suggested applying the procedure described in the International Standard IEC 891 that relates current and voltage of the PV characteristics at given values of temperature and irradiance with the corresponding values at different temperature and irradiance. Moreover, to adapt the diode saturation current I_0 to other temperature conditions, the equation proposed by Townsend [10] can be used. Therefore, based on the corrected value of I_0 and the R_s and R_{sh} values, the rest of the parameters can be extracted using the I_{sc} and V_{oc} values under the new conditions. Following this approach, the parameters that are considered variables under temperature and/or irradiance conditions are I_0, I_{sc} and n. The last parameter, which should be considered independent of temperature, can be evaluated only if I_{mp} and V_{mp} under the new conditions are known; however, this information is usually issued only for standard conditions. Actually, few manufacturers give the maximum power current and voltage temperature coefficients, whereas, it is always unknown how the maximum power point changes with irradiance. For this reason, the quality factor n, which should be used as an adjustment parameter, cannot be evaluated for every value of irradiance and temperature. At any rate, to avoid uncertainty due to the application of corrective methods, De Blas et al. validated their model using recorded data of I_{sc} and V_{oc} under specific temperature and irradiance conditions.

For a mono-crystalline PV module, Celik and Acikgoz [12] performed the experimental verification of the five-parameter model proposed by Hadj Arab and Chenlo [13]. Following the same approach of De Blas et al., the model is based on three equations derived from the Eq. (3) and written in correspondence of the short circuit, the open circuit and maximum power points. The other two equations make the derivative of the Eq. (3), corresponding to the short circuit and the open circuit points, equal to the reciprocal of slopes of the characteristic curve in these points, called R_{sho} and R_{so}. On the basis of the following analytical positions:

$$e^{V_{oc}/nT} \gg 1 \quad R_s \ll R_{sh} \quad I_L \approx I_{sc} \quad \frac{I_0}{nT}e^{I_{sc}R_s/nT} \ll \frac{1}{R_{sh}} \ll \frac{I_0}{nT}e^{V_{oc}/nT} \tag{5}$$

which are usually widely satisfied, the explicit expressions of I_L, I_0, n, R_s and R_{sh} were obtained. As a consequence of Eq. (5), R_{sh} is constant and equal to R_{sho}. To evaluate the PV panel behaviour at a temperature T and irradiance G other than the reference values T_{ref} and G_{ref}, the following expressions were used:

$$I_{sc} = I_{sc,ref}\frac{G}{G_{ref}} + \mu_{I,sc}(T - T_{ref}) \tag{6}$$

$$V_{oc} = V_{oc,ref} + nT\ln\left(\frac{G}{G_{ref}}\right) + \mu_{V,oc}(T - T_{ref}) \tag{7}$$

where $\mu_{I,sc}$ and $\mu_{V,oc}$ are the short circuit current and open circuit voltage temperature coefficients, respectively. As a consequence of the dependence of the explicit expressions of I_L, I_0, n, R_s on Eqs. (6) and (7), these parameters will change if T and/or G are changed. It is easy to verify that Eq. (7) does not perfectly fit the values of V_{oc} that can be read on the I–V characteristics issued by manufacturers. Eq. (7) is based on the following positions:

$$e^{V_{oc,ref}/nT} \gg 1 \quad \frac{V_{oc,ref}}{R_{sh}} \ll I_{L,ref} \quad I_0 = const. \tag{8}$$

The first and the second position are usually satisfied, whereas the third contrasts with the above-mentioned dependence of I_0 on T and G. Moreover, because n is calculated with an expression containing V_{oc}, I_{mp} and V_{mp}, it is not clear how the calculation of n could be performed because V_{oc} depends on n itself and usually on the values of I_{mp} and V_{mp}, as the generic irradiance is not known.

Despite Eqs. (5) and (8), on which the last two methods are based, these methods allow a good representation of the SRC characteristic. Unfortunately, as will be shown in the following, some inaccuracies are evident when the characteristics are calculated with an irradiance other than 1000 W/m^2.

4. A new five-parameter model

The five-parameter model proposed is described by the following equation:

$$I(\alpha_G,T) = \alpha_G I_L(T) - I_0(\alpha_G,T)\left(e^{(\alpha_G[V+KI(T-T_{ref})]+IR_s)/\alpha_G nT} - 1\right) - \frac{\alpha_G[V+KI(T-T_{ref})]+IR_s}{R_{sh}} \tag{9}$$

where the quantity $\alpha_G = G/G_{ref}$ denotes the ratio between the generic solar irradiance and the solar irradiance at SRC. K is a thermal correction factor similar to the curve correction factor described by the IEC 891, and the photocurrent $I_L(T)$ can be evaluated with the relation

$$I_L(T) = I_{L,ref} + \mu_{I,sc}(T - T_{ref}) \tag{10}$$

where $I_{L,ref}$ is the value of the photocurrent at SRC. The parameters n, R_s and R_{sh} are constant for each temperature and irradiance. For the sake of simplicity, the expression of the quantity $I_0(\alpha_G,T)$, which describes the way the reverse saturation current changes with the solar irradiance and temperature, will be shown in the following. Obviously, at SRC, it is $\alpha_G = 1$, $T = T_{ref}$, and Eq. (9) becomes equal to the traditional five-parameter Eq. (3).

The procedure to determine the parameters of the model requires the preliminary estimation of R_{sho} and R_{so}, which are the reciprocal of slopes of the characteristic I–V curve at SRC corresponding to the short circuit and open circuit points, respectively. The knowledge of $I_{sc,ref}$, $V_{oc,ref}$, $I_{mp,ref}$ and $V_{mp,ref}$ at SRC and of V_{oc} at the standard temperature and at the lowest available irradiance (usually 200 W/m^2) and $T = T_{ref}$ are also needed. For the determination of K, the values of I_{mp} and V_{mp} at a temperature other than T_{ref} (usually 75 °C) and at $G = 1000$ W/m^2 are necessary. All these data can be easily extracted from the I–V curves provided by manufacturers. On the basis of this

information the following positions are made for SRC:

- short circuit point: $V=0$ $I=I_{sc,ref}$

$$I_{sc,ref}=I_{L,ref}-I_{0,ref}(e^{I_{sc,ref}R_s/nT_{ref}}-1)-\frac{I_{sc,ref}R_s}{R_{sh}} \tag{11}$$

- derivative at the short circuit point

$$\left.\frac{dI}{dV}\right|_{\substack{V=0\\I=I_{sc,ref}}}=-\frac{(I_{0,ref}/nT_{ref})e^{I_{sc,rfe}R_s/nT_{ref}}+1/R_{sh}}{1+R_s((I_{0,ref}/nT_{ref})e^{I_{sc,ref}R_s/nT_{ref}}+1/R_{sh})}=-\frac{1}{R_{sho}} \tag{12}$$

- open circuit point: $V=V_{oc,ref}$ $I=0$

$$0=I_{L,ref}-I_{0,ref}(e^{V_{oc,ref}/nT_{ref}}-1)-\frac{V_{oc,ref}}{R_{sh}} \tag{13}$$

- derivative at the open circuit point

$$\left.\frac{dI}{dV}\right|_{\substack{V=V_{oc,ref}\\I=0}}=-\frac{(I_{0,ref}/nT_{ref})e^{V_{oc,ref}/nT_{ref}}+1/R_{sh}}{1+R_s(I_{0,ref}/nT_{ref}e^{V_{oc,ref}/nT_{ref}}+1/R_{sh})}=-\frac{1}{R_{so}} \tag{14}$$

- maximum power point: $V=V_{mp,ref}$ $I=I_{mp,ref}$

$$I_{mp,ref}=I_{L,ref}-I_{0,ref}(e^{(V_{mp,ref}+I_{mp,ref}R_s)/nT_{ref}}-1)-\frac{V_{mp,ref}+I_{mp,ref}R_s}{R_{sh}} \tag{15}$$

The resolution of this equations system was initially attempted using special tools, like Mathematica and MATLAB, but unfortunately, no valid solution was achieved. The system was solved by a numeric algorithm based on a double process of trial and error for the parameters R_s and n, with the second process nested into the first. To start the process, it is necessary to use the following conditions:

$$I_{L,ref}=I_{sc,ref} \quad R_{sh}=R_{sho} \tag{16}$$

obtained by Eqs. (12) and (13) under the usually widely satisfied conditions

$$R_s \ll R_{sho} \quad \frac{I_{0,ref}}{nT_{ref}}e^{I_{sc,ref}R_s/nT_{ref}} \ll \frac{1}{R_{sh}} \tag{17}$$

Once some first attempt values for R_s and n of Eq. (16) are set, the current $I_{0,ref}$, the photocurrent $I_{L,ref}$ and the resistance R_{sh} are calculated in sequence with Eqs. (15), (11) and (12), respectively. Once these parameters are determined, through Eq. (13), the

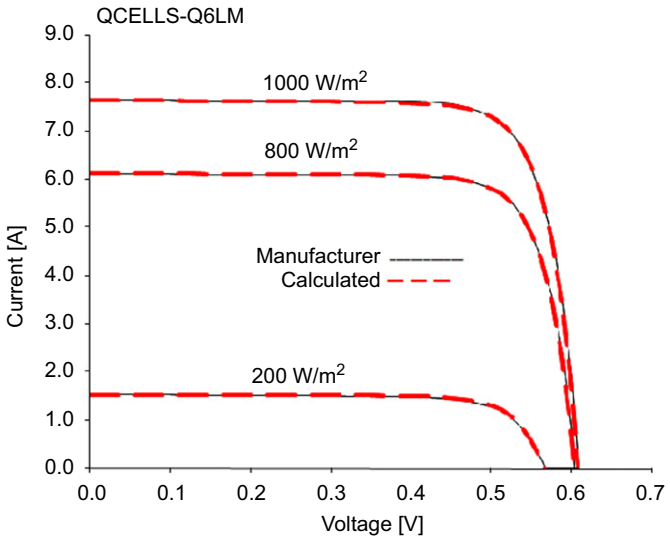

Fig. 3. Comparison between calculated (new model) and issued current–voltage characteristics of Q6LM at temperature $T=25$ °C.

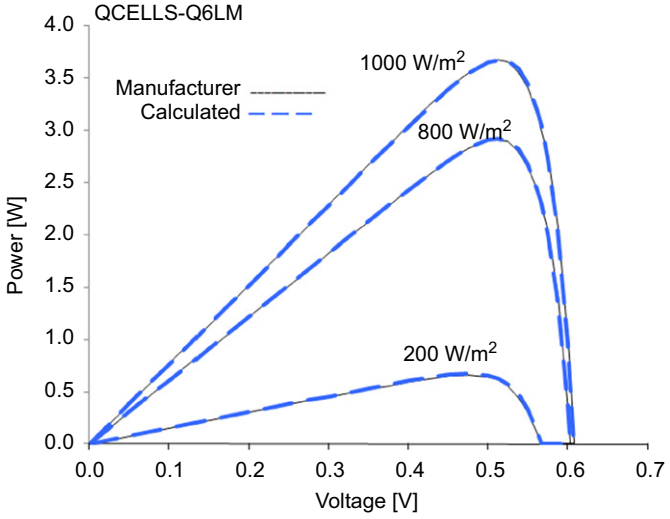

Fig. 4. Comparison between calculated (new model) and issued power–voltage characteristics of Q6LM at temperature $T=25$ °C.

Table 1
Data for the evaluation of the cell model parameters.

Temperature	25 °C						
Irradiance	1 kW/m^2						0.2 kW/m^2
Cell type	V_{oc} (V)	I_{sc} (A)	V_{mp} (V)	I_{mp} (A)	R_{sho} (Ω)	R_{so} (Ω)	V_{oc} (V)
Qcells Q6LM	0.608	7.665	0.513	7.174	9.967	0.00443	0.567

Table 2
Evaluated model parameters of the cell

Temperature	25 °C					
Irradiance	1 kW/m^2					0.2 kW/m^2
Cell type	I_L (A)	I_0 (A)	n (V/K)	R_{sh} (Ω)	R_s (Ω)	I_0 (A)
Qcells Q6LM	7.65549	7.87236×10^{-8}	1.10920×10^{-4}	9.9672	7.7315×10^{-5}	5.44241×10^{-8}

value of n is recalculated, compared with the first attempt value and adequately changed. This first trial and error process is reiterated until the convergence of n is achieved with the desired accuracy. Then, R_s is evaluated by means of Eq. (14) and compared to the first attempt value of R_s. On the basis of this comparison the second trial and error process is carried out: R_s is changed, again the first trial and error process is performed on n, a new value of R_s is set, and the procedure is carried on to obtain the convergence of the results. In this way, the five equations are solved in a non-approximate form because no simplification is used.

The above procedure, which can be easily coded into a short software routine using simple languages, finds the solution of the equations system with the desired accuracy without to the need for guidance towards solutions starting from fitted initial values of the searched parameters. In particular, as implemented in VBA macros in Microsoft Excel, it provides the most accurate results with a rapid convergence.

In order to understand how the series and shunt resistances are affected by the solar irradiance, the previous equation system was solved for several values of G. In particular, the data collected from the I–V curves provided by manufacturers and referred to many PV panels at the standard temperature and at irradiances included between 200 and 1000 W/m^2 were used. The analysis made it possible to observe that both the series and the shunt resistance seem to vary in almost inverse linear mode with the

Table 3
Absolute mean current & power differences at temperature $T=25$ °C.

PV Cell	Absolute mean difference	Irradiance (W/m^2)		
		200	800	1000
Qcells Q6LM	Current (A)	0.021	0.023	0.026
	Power (W)	0.009	0.010	0.014

Table 4
Data for the evaluation of the model parameters.

Irradiance	1 kW/m^2										0.2 kW/m^2
Temperature	25 °C						75 °C		25÷75 °C		25 °C
Panel type	V_{oc} (V)	I_{sc} (A)	V_{mp} (V)	I_{mp} (A)	R_{sho} (Ω)	R_{so} (Ω)	V_{mp} (V)	I_{mp} (A)	$\mu_{V,oc}$ (V/°C)	$\mu_{I,sc}$ (A/°C)	V_{oc} (V)
Kyocera KC175GHT-2	29.35	8.07	23.60	7.57	99.44	0.42	18.00	7.50	-1.07×10^{-1}	2.22×10^{-3}	27.20
Sanyo HIP-180BA19	66.40	3.66	52.00	3.51	3920.0	2.90	45.00	3.44	-1.66×10^{-1}	6.81×10^{-4}	61.60

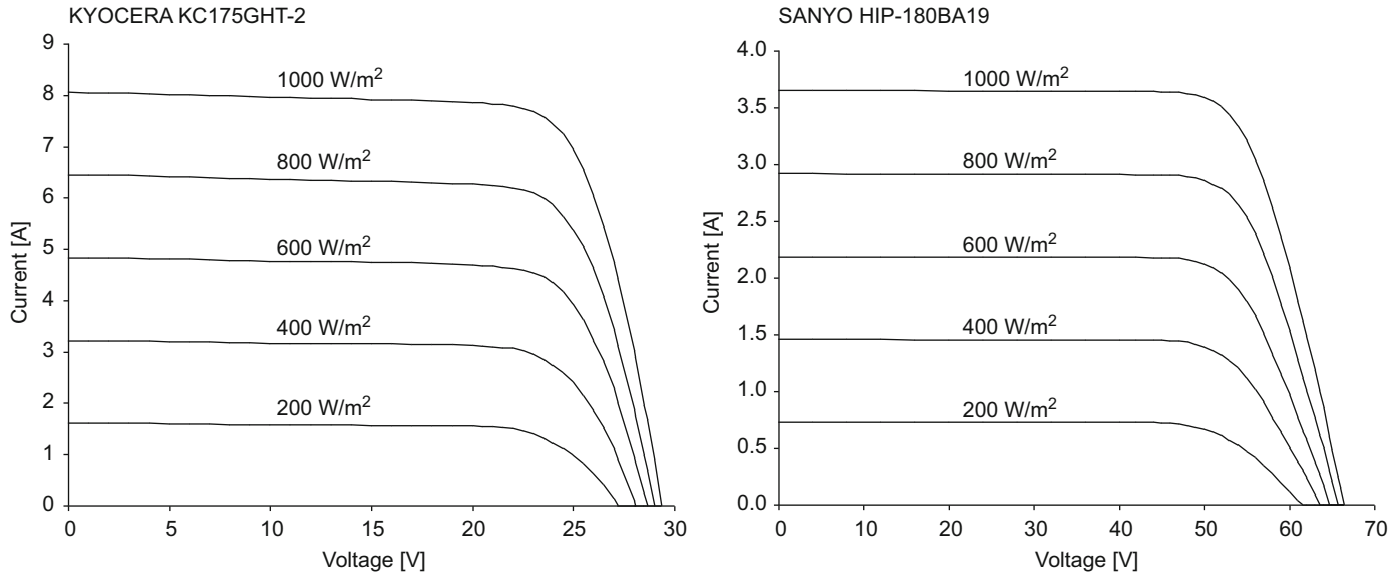

Fig. 5. Current–voltage characteristics of KC175GHT-2 and of HIP-180 BA19 at temperature $T=25$ °C.

Table 5
Evaluated model parameters.

Irridance	1 kW/m^2						0.2 kW/m^2
Temperature	25 °C					25÷75 °C	25 °C
Panel type	I_L (A)	I_0 (A)	n (V/K)	R_{sh} (Ω)	R_s (Ω)	K (Ω/°C)	I_0 (A)
Kyocera KC175GHT-2	8.09277	9.60241×10^{-12}	3.58974×10^{-3}	99.158	0.282	1.12182×10^{-3}	1.4356×10^{-11}
Sanyo HIP-180BA19	3.65813	3.61724×10^{-16}	6.04394×10^{-3}	3917.592	2.408	-5.36333×10^{-3}	1.03845×10^{-15}

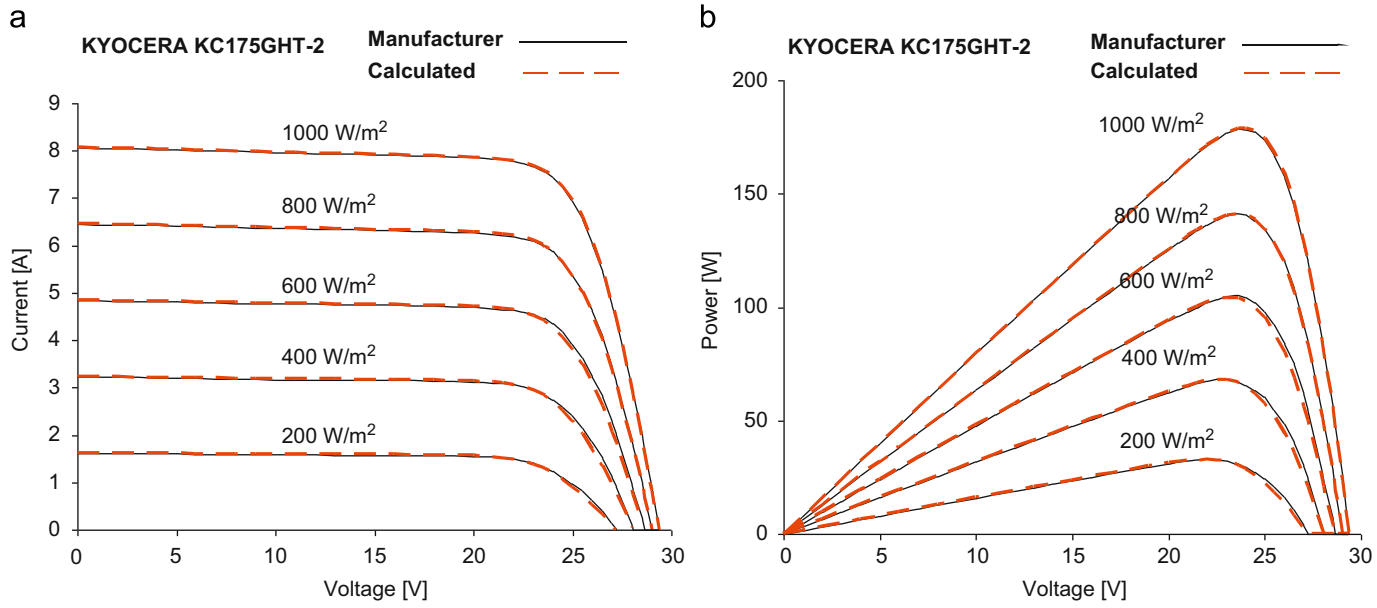

Fig. 6. Comparison between calculated (new model) and issued current–voltage and power–voltage characteristics of KC175GHT-2 at temperature $T=25$ °C.

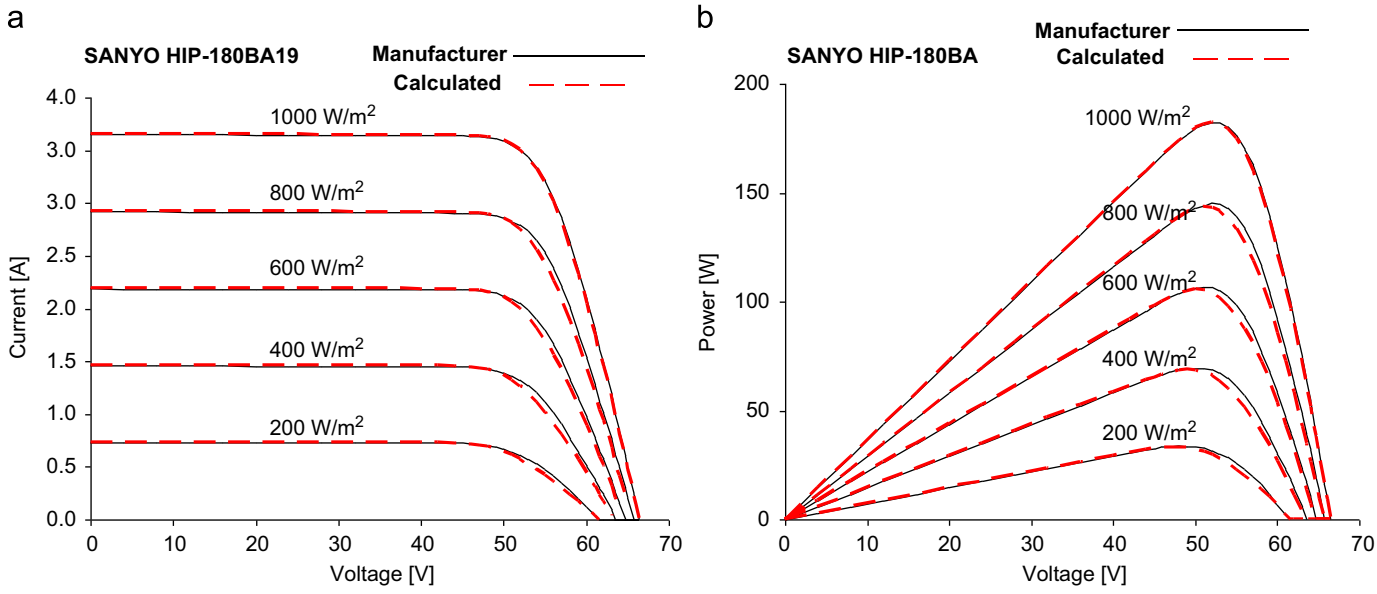

Fig. 7. Comparison between calculated (new model) and issued current–voltage and power–voltage characteristics of HIP-180 BA19 at temperature $T=25$ °C.

solar irradiance:

$$R_s(\alpha_G)=\frac{R_s}{\alpha_G} \quad R_{sh}(\alpha_G)=\frac{R_{sh}}{\alpha_G} \tag{18}$$

where the values of the resistances R_s and R_{sh} are evaluated in SRC. By means of Eq. (18) and with simple manipulations, Eq. (3) can be rewritten in the form of Eq. (9), which contains constant values of R_s and R_{sh}.

Another significant observation concerns the current $I_0(\alpha_G, T)$, whose value, for the each irradiance and temperature, can be calculated by using the relation

$$I_0(\alpha_G,T)=\alpha_G\left(\frac{I_L(T)-V_{oc}(\alpha_G,T)/R_{sh}}{e^{V_{oc}(\alpha_G,T)/nT}-1}\right) \tag{19}$$

obtained by Eq. (9) written for the open circuit point. In Eq. (19) the $V_{oc}(\alpha_G,T)$ referring to the generic values of G and T must be used. While the variation of I_L and V_{oc} with the temperature, at constant irradiance, can be evaluated with Eq. (10) and with the relation

$$V_{oc}(\alpha_G,T)=V_{oc,ref}(\alpha_G)+\mu_{V,oc}(T-T_{ref}) \quad G=const. \tag{20}$$

respectively, a reliable expression of $V_{oc,ref}(\alpha_G)$, relating the open circuit voltage with the solar irradiance, is not available. Actually, expressions like Eq. (7) or similar, do not have the desired accuracy.

The calculations of the current $I_0(\alpha_G,T)$ performed with Eq. (19) on the basis of the data collected from the I–V curves provided by

manufacturers and referred to several PV panels at the standard temperature and at the irradiances included between 200 and 1000 W/m^2 show a regular dependence of the reverse saturation current on the solar irradiance. With a good approximation, the reverse saturation current can be expressed by the following equation:

$$I_0(\alpha_G,T)=\exp\left[\left(\frac{\alpha_G-0.2}{1-0.2}\right)\ln\frac{I_0(1,T)}{I_0(0.2,T)}+\ln I_0(0.2,T)\right] \quad (21)$$

obtained by interpolating, in a logarithmic mode, the value of $I_0(1,T)$, calculated with Eq. (19) for $G=G_{ref}=1000$ W/m^2 ($\alpha_G=1$), with $I_0(0.2,T)$ calculated for $G=200$ W/m^2 ($\alpha_G=0.2$). Once the values of I_{sc} and V_{oc} are evaluated with Eqs. (10) and (20) for the required temperature T at the solar irradiances of 1000 and 200 W/m^2, the values of $I_0(1,T)$ and $I_0(0.2,T)$ can be calculated with Eq. (19) and then used in Eq. (21) to determine $I_0(\alpha_G,T)$.

The thermal correction factor K is used to slide the I–V characteristic at irradiance G_{ref} on the V axis in order to better fit the characteristics issued by the manufacturer at temperatures T^* different than T_{ref}. This factor can be calculated with the formal imposition that the I–V characteristic evaluated with Eq. (9) at G_{ref} and at the desired temperature T^* must contain the maximum power point issued by the manufacturer for the same T^*:

$$K=\frac{V_{mp}-V^*_{mp}}{I^*_{mp}(T^*-T_{ref})} \quad (22)$$

where V^*_{mp} and I^*_{mp} are the coordinates of maximum power point at $T=T^*$ issued by the manufacturer, and V_{mp} is the voltage in correspondence of the maximum power point evaluated with Eq. (9) setting $K=0$. The value of T^* to be used to determine K should be chosen by considering the maximum or the minimum expected working temperature of the PV module and, obviously, the data provided by the manufacturer. In this paper a temperature of $T^*=75$ °C was used.

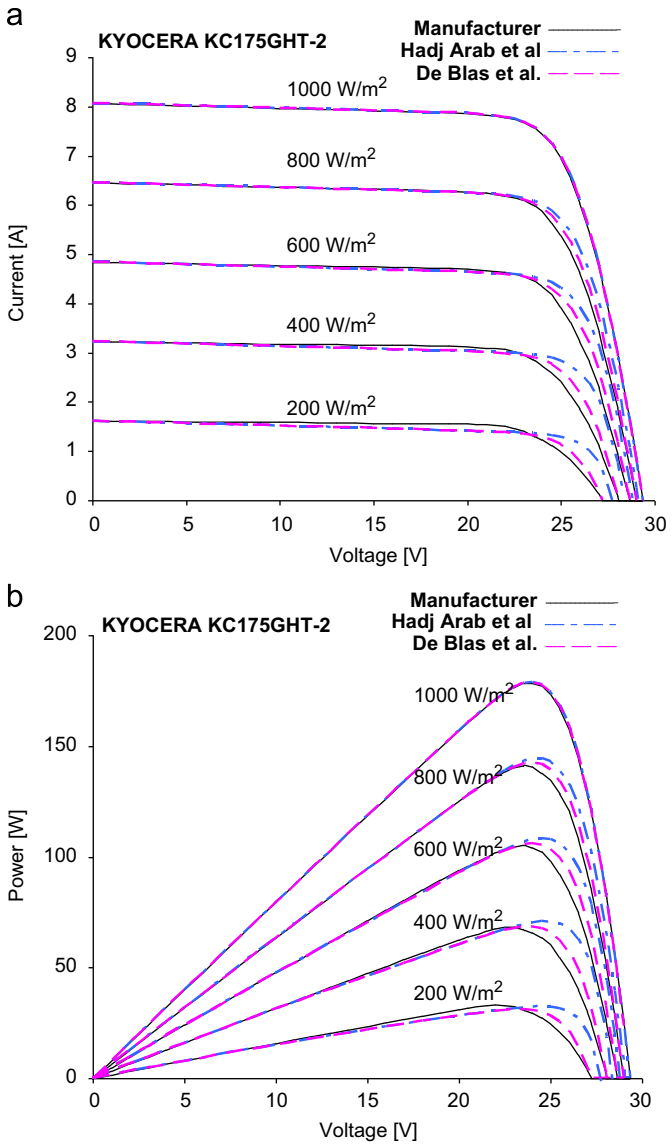

Fig. 8. (a) Comparison between calculated (De Blas et al. and Hadj Arab et al. models) and issued current–voltage characteristics of KC175GHT-2 at temperature $T=25$ °C. (b) Comparison between calculated (De Blas et al. and Hadj Arab et al. models) and issued power–voltage characteristics of KC175GHT-2 at temperature $T=25$ °C.

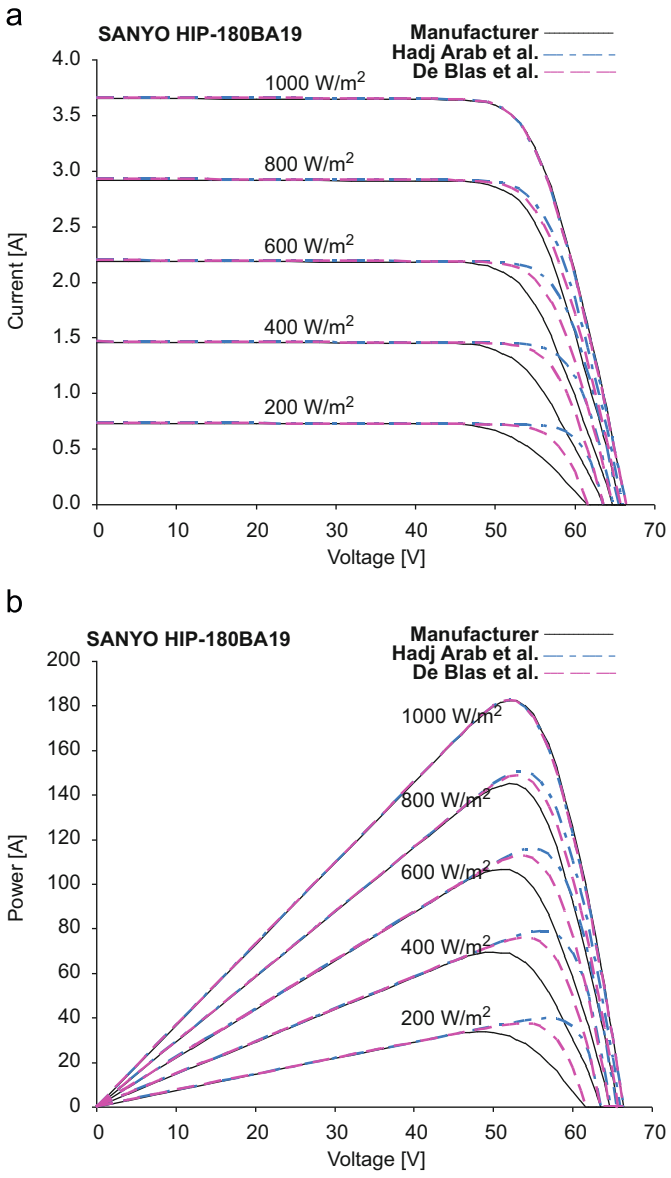

Fig. 9. (a) Comparison between calculated (De Blas et al. & Hadj Arab et al. models) and issued current-voltage characteristics of HIP-180 BA19 at temperature $T=25$ °C. (b) Comparison between calculated (De Blas et al. and Hadj Arab et al. models) and issued power-voltage characteristics of HIP-180 BA19 at temperature $T=25$ °C.

5. Application of the new model and analysis of the results

Before verifying the capability of the proposed model to fit PV panel characteristics, a test on a single solar cell in SRC at AM 1.5 was conducted. The model was used to represent the *I–V* characteristics of a QCELLS mod. Q6LM with the performance data of Table 1; the calculated values of the parameters are reported in Table 2. The model effectiveness is evident in Figs. 3 and 4 in which the issued and the calculated characteristics are compared. The model is very accurate and represents the cell characteristics with the small absolute mean differences of current and power that are listed in Table 3. Unfortunately, the *I–V* curves of cells at temperature different from 25 °C are usually not issued by manufacturers and for this reason the thermal performance of the model was not tested.

More exhaustive tests have been conducted on PV panels whose *I–V* curves at temperature different from 25 °C are issued by the best manufacturers. The procedure described above was used for two panels built with a different processing technology and with the performance data shown in Table 4. Such parameters can be slightly different than those issued by the manufacturers; actually, for the sake of accuracy, some of these parameters were directly extracted from the *I–V* characteristics. In Fig. 5 the *I–V* characteristics of the panels are reported. Both panels have quite the same maximum power and, due to their good quality, also have similarly high fill factor values (≈ 0.75). At first glance, the curves seem to be quite similar, but if more accurately examined, they show some differences, probably due to their different processing technology. In particular, the Sanyo panel curves are more linear and, for low voltages, also almost horizontal.

By applying the procedure described in the previous paragraph, the parameters of the equivalent electrical circuit in Table 5 were obtained. The comparison between the data in Table 5 shows that panels with similar power performance may be described by parameters with extremely different values. In particular, many orders of magnitude separate the values of the reverse saturation current, which is the parameter that mainly affects the shape of the *I–V* characteristics near the maximum power point. For this reason, it is very common that the solution of Eqs. (11)–(15), performed with powerful mathematical tools, succeeds only if it is appropriately guided.

In Figs. 6 (a), (b), 7 (a), and (b), the current–voltage and power–voltage curves evaluated with the calculated parameters are compared with the characteristics issued by manufacturers. Figs. 6 (a), (b), 7(a), and (b) show a good agreement between the provided and calculated data. Some little inaccuracies still occur for voltages greater than the maximum power voltage, but the new model works better than those proposed by other authors [11,12]. To prove what was claimed, the characteristics of the panels were drawn on the basis of the results obtained by the methods described here. In particular, to apply the method of De Blas et al., it was necessary to use the values of V_{oc} extracted from the characteristics issued by the manufacturers because the other indicated procedures did not allow an adequate accuracy. This point represents a lack of generality for the method. Moreover, because of the previously mentioned difficulty in evaluating the value of n related to the generic irradiance, the model of Hadj Arab et al. was used while assuming the constant value of n calculated in SRC. The results of such evaluations are reported in Figs. 8 (a), (b), 9 (a), and (b).

It is easy to see that even though all the procedures adequately fit the curve drawn for $G=1000\ \mathrm{W/m^2}$, the new model better represents the characteristics of both panels at $G \neq G_{ref}$. Actually, the De Blas et al. and Hadj Arab et al. models overestimate the power for voltage values greater than the maximum power point voltage. With the Kyocera panel, an underestimation of the power can also be observed due to the fact that a constant value was used for the shunt resistance. It is known that R_{sh} mainly affects the slope of the characteristics for voltage values smaller than the

Table 6
Absolute mean current and power differences between the issued and the calculated *I–V* characteristics at temperature $T=25$ °C.

PV panel	Absolute mean difference	Irradiance ($\mathrm{W/m^2}$)				
		200	400	600	800	1000
KC175GHT-2	Current (A)	0.021	0.032	0.045	0.018	0.016
	Power (W)	0.480	0.773	1.142	0.406	0.392
HIP-180 BA19	Current (A)	0.016	0.032	0.034	0.042	0.014
	Power (W)	0.826	1.784	1.878	2.430	0.826

Table 7
Maximum current and power differences between the issued and the calculated *I–V* at temperature $T=25$ °C.

Parameters at the maximum difference points			Irradiance ($\mathrm{W/m^2}$)				
			200	400	600	800	1000
Kyocera KC175GHT-2	Current difference	Voltage (V)	26.0	26.5	27.0	26.5	29.0
		Issued current (A)	0.629	1.508	2.288	4.073	0.895
		Calculated current (A)	0.535	1.344	2.062	4.001	0.820
		Difference (A)	−0.094	−0.164	−0.226	−0.072	−0.075
	Power difference	Voltage (V)	26.0	27.0	27.0	26.5	29.0
		Issued current (A)	0.629	1.106	2.288	4.073	0.895
		Calculated current (A)	0.535	0.942	2.062	4.001	0.820
		Issued power (W)	16.354	29.862	61.776	107.935	25.955
		Calculated power (W)	13.910	25.434	55.674	106.027	23.780
		Difference (W)	−2.444	−4.428	−6.102	−1.908	−2.175
Sanyo HIP-180 BA19	Current difference	Voltage (V)	54.0	57.0	56.0	58.0	63.0
		Issued current (A)	0.529	0.906	1.662	2.006	1.182
		Calculated current (A)	0.474	0.808	1.562	1.879	1.133
		Difference (A)	−0.055	−0.098	−0.100	−0.127	−0.049
	Power Difference	Voltage (V)	54.0	57.0	57.0	58.0	63.0
		Issued current (A)	0.529	0.906	1.509	2.006	1.182
		Calculated current (A)	0.474	0.808	1.411	1.879	1.133
		Issued power (W)	28.566	51.642	86.013	116.348	74.466
		Calculated power (W)	25.596	46.056	80.427	108.982	71.379
		Difference (W)	−2.970	−5.586	−5.586	−7.366	−3.087

maximum power point voltage. When R_{sh} has a small value, Eq. (18) should be more sensitive to the irradiance, and a constant value of R_{sh} will yield greater inaccuracy. On the other hand, the new model shows a little underestimation of the power, which will lead to more cautious results and wiser predictions when the model is used to simulate the behaviour of a PV system and to evaluate the benefit of the economic investment.

For the analysed panels, Table 6 provides the absolute mean differences of current and of power between the issued and the calculated data. Table 7 lists the maximum differences of current and of power between the issued and the calculated data. At constant temperature, the absolute mean differences for the current and for the power do not exceed 0.045 A and 2.430 W, respectively. The maximum current difference is −0.226 A, and the maximum power difference is −7.366 W.

Besides verifying the accuracy of the PV models to fit with the solar irradiance, it is also very important to analyse their capabilities to reproduce the way PV panel performance is affected by the silicon temperature. It is well known that the efficiency of a PV panel dramatically drops when the temperature increases, and this drop usually occurs when the solar radiation reaches the greatest values. As a consequence, because the energy globally produced during a day is mainly affected by the solar energy collected in the presence of the daily highest irradiance values, if the model is inaccurate, unrealistic economic returns will be predicted. Unfortunately, that is a weakness of the method because the data related to the PV panel thermal behaviour, which are issued by the manufacturers, are insufficient and do not allow reliable predictions. Usually, the best information concerns the short circuit current and open circuit voltage temperature coefficients, the curve correction factor, defined by IEC 891, and the I–V characteristics at $G=1000\ \mathrm{W/m^2}$ for some fixed temperature values.

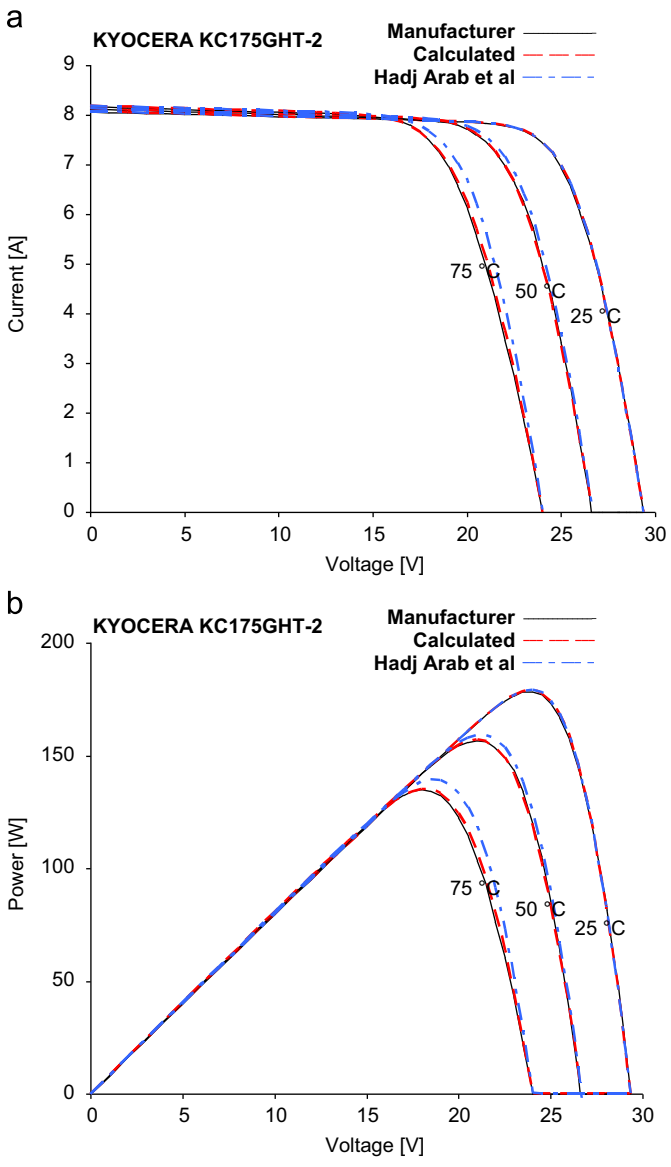

Fig. 10. (a) Comparison between calculated (new model & Hadj Arab et al. model) and issued current-voltage characteristics of KC175GHT-2 at irradiance $G=1\ \mathrm{kW/m^2}$. (b) Comparison between calculated (new model and Hadj Arab et al. model) and issued power-voltage characteristics of KC175GHT-2 at irradiance $G=1\ \mathrm{kW/m^2}$.

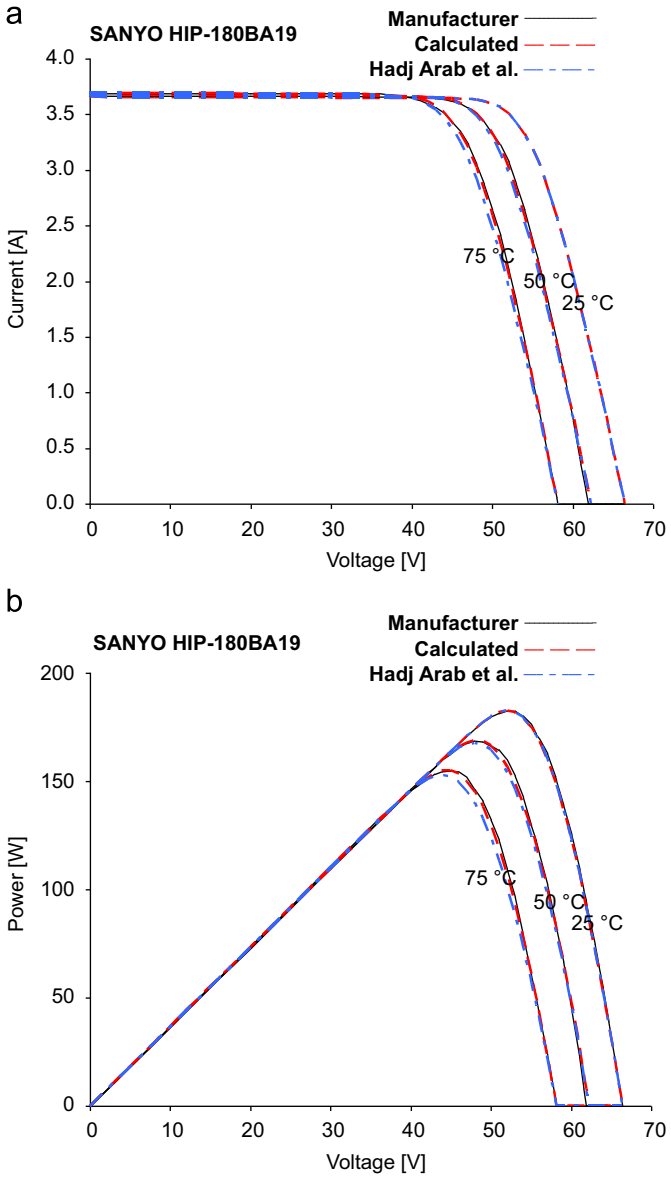

Fig. 11. (a) Comparison between calculated (new model & Hadj Arab et al. model) and issued current-voltage characteristics of HIP-180 BA19 with at irradiance $G=1\ \mathrm{kW/m^2}$. (b) Comparison between calculated (new model and Hadj Arab et al. model) and issued power–voltage characteristics of HIP-180 BA19 with at irradiance $G=1\ \mathrm{kW/m^2}$.

The new model was used to evaluate the current–voltage and the power–voltage curves of the two PV panels analysed, and the results were compared with the data issued by manufacturers and with those ones calculated with the procedure of Hadj Arab et al. It was impossible to use the model of De Blas et al. because the trial and error process did not converge when the saturation current was evaluated with the Townsend equation. Figs. 10 (a), (b), 11 (a), and (b) compare the calculations. For the analysed panels, Table 8 provides the absolute mean differences of current and of power between the issued and the calculated data. Table 9 lists the maximum differences of current and of power between the issued and the calculated data. At constant irradiance the absolute mean differences for the current and for the power do not exceed 0.041 A and 1.378 W, respectively. The maximum current difference is 0.190 A, and the maximum power difference is 6.283 W.

Due to the similar approach for evaluating the dependence of the reverse saturation current on the temperature, the model of Hadj Arab et al. and the new model both give a good representation of the PV panel curves for different temperature values. Actually, the new model is slightly more accurate for the use of the coefficient K, which reaches the goal of a suitable slide of the I–V characteristics.

With Figs. 6–9 (b), it is easy to see that because the models evaluate diverse power curves, some significant differences in the power calculations may be expected if the irradiance varies from zero to 1000 W/m^2. On the contrary, in Figs. 10 and 11 (b), the evaluated curves are quite similar; thus, a smaller dependence on the temperature is expected for the calculated power. Actually, Figs. 6–11 do not allow an easy estimation of the PV panel behaviour when both the solar irradiance and the silicon temperature are changing; however, it is interesting to see how the differences between the characteristics drawn in the previous figures affect the accuracy of the results.

To investigate further, the model of Hadj Arab et al. and the new model were used to evaluate the electrical power by assuming the values drawn in Fig. 12 for the irradiance and the temperature that realistically represent the working conditions of a PV panel during a summer sunny day in the south of Italy.

The electrical power also depends on R_L connected to the panel because the load defines the operating point on the I–V characteristic plane. For given values of irradiance, temperature and electrical load, the operating point can be determined by solving the system of equations formed by the PV panel characteristic $I=f(V)$ and by the electrical load characteristic $I=V/R_L$. Such a solution, if R_L is constant, can be easily achieved with a graphical method by drawing a straight line with a slope inversely proportional to R_L on the I–V characteristic plane. The intersection of the straight line and the PV panel characteristic

Table 8
Absolute mean current and power differences between the issued and the calculated I–V characteristics at irradiance $G=1$ kW/m^2.

PV panel	Absolute mean difference	Temperature (deg.)		
		25	50	75
KC175GHT-2	Current (A)	0.015	0.025	0.041
	Power (W)	0.383	0.561	0.818
HIP-180 BA19	Current (A)	0.015	0.025	0.017
	Power (W)	0.864	1.378	0.820

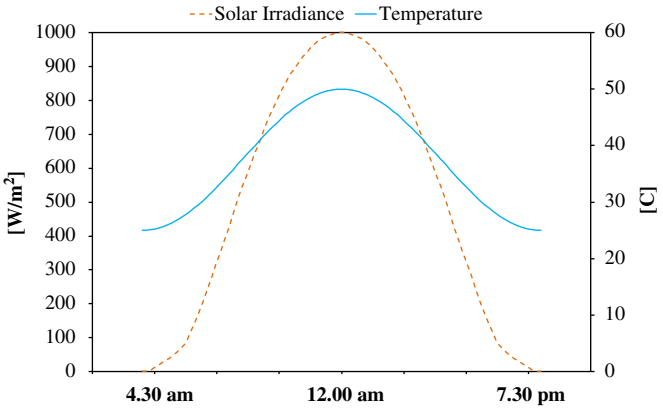

Fig. 12. Solar irradiance and silicon temperature profiles used to calculate the electrical power.

Table 9
Maximum current and power differences between the issued and the calculated I–V characteristics at irradiance $G=1$ kW/m^2.

Parameters at the maximum difference point			Temperature (°C)		
			25	50	75
Kyocera KC175GHT-2	Current difference	Voltage (V)	29.0	24.5	22.0
		Issued current (A)	0.895	4.290	3.462
		Calculated current (A)	0.820	4.187	3.652
		Difference (A)	−0.075	−0.103	0.190
	Power difference	Voltage (V)	29.0	24.5	22.0
		Issued current (A)	0.895	4.290	3.462
		Calculated current (A)	0.820	4.187	3.652
		Issued power (W)	25.955	105.105	76.164
		Calculated power (W)	23.780	102.582	80.344
		Difference (W)	−2.175	−2.523	4.180
Sanyo HIP-180 BA19	Current difference	Voltage (V)	61.9	61.6	51.0
		Issued current (A)	1.529	0.128	2.409
		Calculated current (A)	1.479	0.230	2.331
		Difference (A)	−0.050	0.102	−0.078
	Power difference	Voltage (V)	61.9	61.6	51.0
		Issued current (A)	1.529	0.128	2.409
		Calculated current (A)	1.479	0.230	2.331
		Issued Power (W)	94.645	7.885	122.859
		Calculated Power (W)	91.550	14.168	118.881
		Difference (W)	−3.095	6.283	−3.978

corresponds to the working point sought. The same method can be used to draw the curve of the electrical load power $P=V^2/R_L$ on the power–voltage characteristics plane. Referring to the Kyocera KC175GHT-2 panel, the curves of the electrical load power, for some values of R_L, are shown in the Fig. 13, which is derived from Figs. 6 (b), 8 (b) and 10 (b).

Due to the presence of the constant electrical load R_L, the PV panel will work at operating points that are on the power–voltage characteristic corresponding to the chosen value of R_L. That curve will be travelled up and down because the operating point position will also depend on the current values of the irradiance and of the temperature. The electrical powers evaluated for four different values of R_L using the Hadj Arab et al. model and the new model are shown in Figs. 14–17. As expected, the differences between the two models are more evident when the value of the electrical load is greater. On the contrary, it seems strange that the maximum power value is not reached at the maximum irradiation. Actually, since lowering the temperature tends to increase the electrical power due to a counterbalancing effect, almost similar power values can be achieved for high values of irradiance and temperature as well as for low values of the same physical parameters. This effect is clearly shown in Figs. 16 and 17, where the power evaluated by the Hadj Arab et al. model far from noon, where $G=1000\ W/m^2$ and $T=50\ ^\circ C$, is even smaller than the one calculated before and after 12.00 a.m. For $R_L=18\ \Omega$ the power for $G=544\ W/m^2$ and $T=37.5\ ^\circ C$ is 4.44% higher than the one produced at noon. Even though the new model confirms the presence of the counterbalancing effect described above, its behaviour is always more moderate.

Unfortunately, the data issued by the manufacturers are insufficient to make a true judgment about the capability of the models to represent the PV panel thermal behaviour with changing irradiance and temperature. Actually, more data or

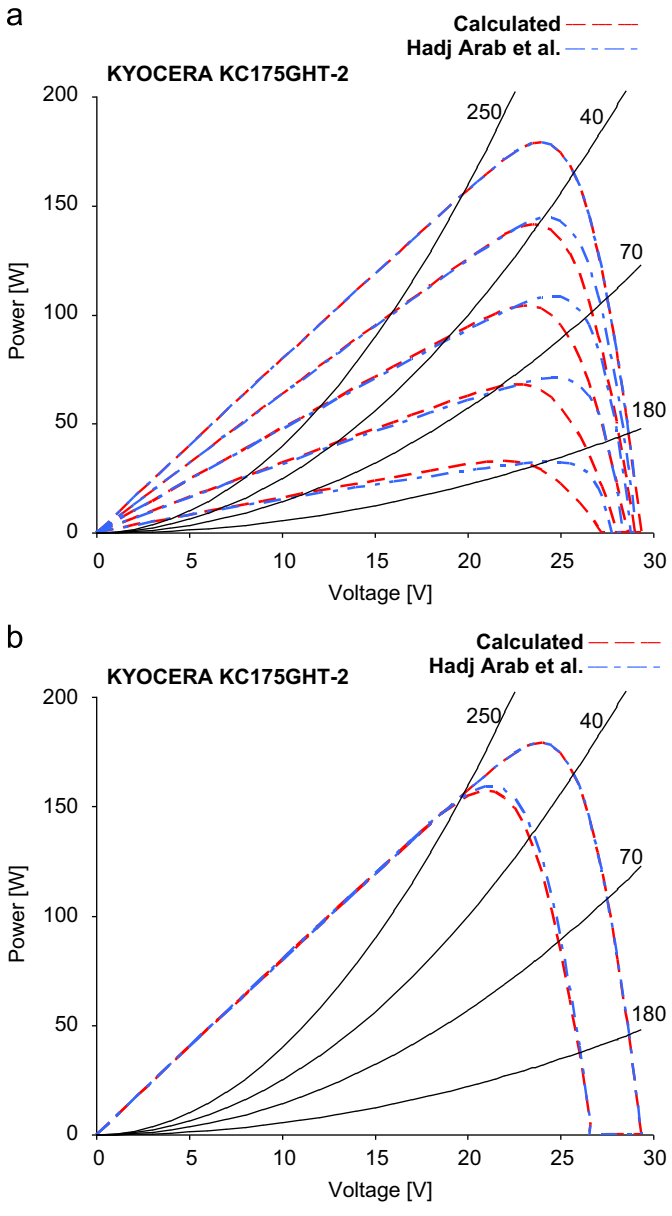

Fig. 13. (a) Electrical load, Hadj Arab et al., and new model power–voltage characteristics at $T=25\ ^\circ C$ for PV panel Kyocera KC175GHT-2. Fig. 13(b). Electrical load, Hadj Arab et al., and new model power-voltage characteristics at $G=1000\ W/m^2$ for PV panel Kyocera KC175GHT-2.

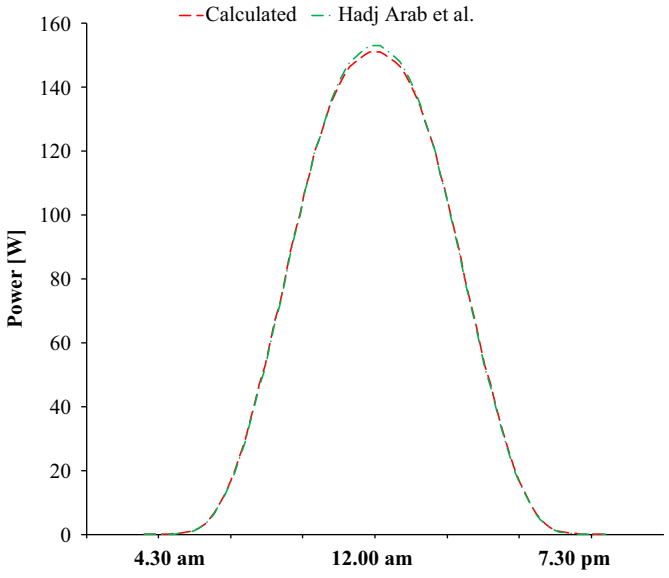

Fig. 14. Electrical power evaluated with $R_L=2.5\ \Omega$.

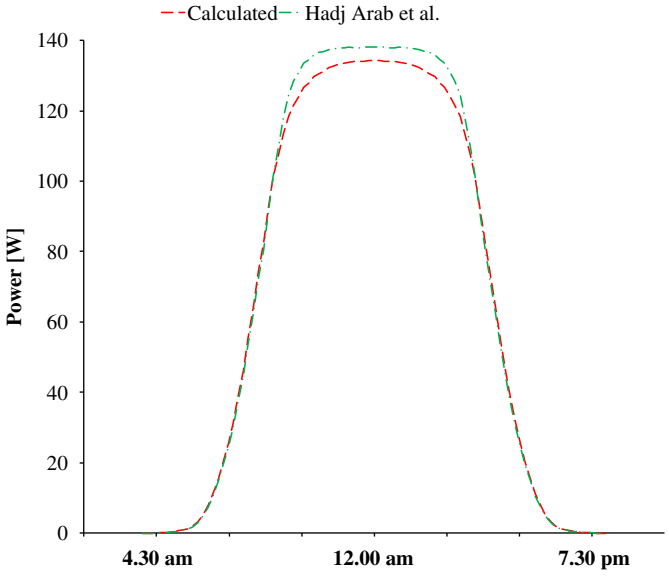

Fig. 15. Electrical power evaluated with $R_L=4\ \Omega$.

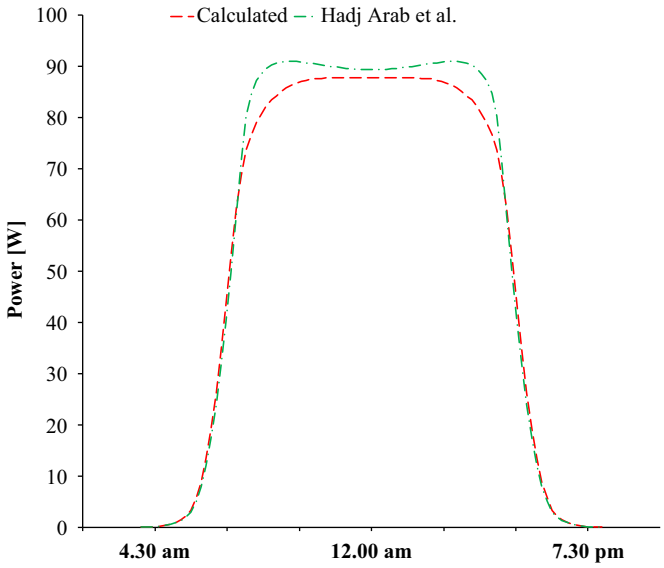

Fig. 16. Electrical power evaluated with $R_L=7\ \Omega$.

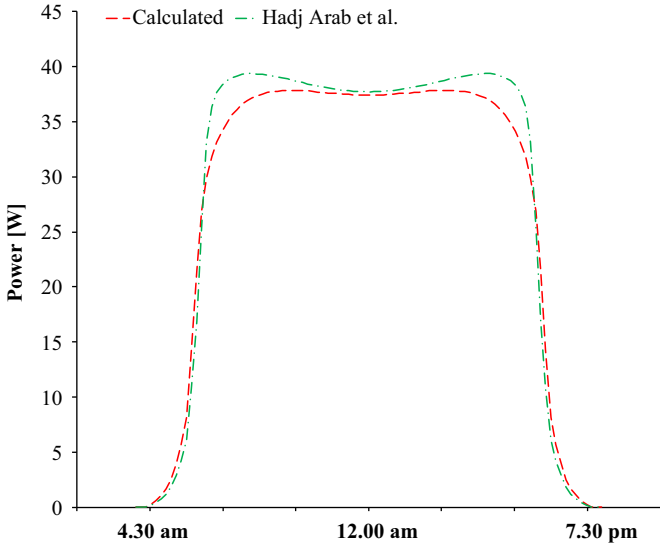

Fig. 17. Electrical power evaluated with $R_L=18\ \Omega$.

experimental validations are needed, but this topic is beyond the goal of the present paper.

6. Conclusions

The new method allows for the determination of the electrical parameters of a PV panel and the assessment of the power generated for any conditions of operating temperature and solar irradiance. Starting from the one-diode electrical equivalent circuit, a system of five equations, which uses only data commonly provided by manufacturers, was numerically solved without any approximation or simplification that may affect the reliability of the results.

The five parameters R_s, R_{sh}, n, I_L and I_0 are obtained by imposing on both the calculated I–V characteristics and those issued by manufacturers the following conditions: equality of the short circuit current, equality of the open circuit voltage, correspondence of the maximum power point and equal values of the curve derivative in the points of short circuit and open circuit for nominal conditions. Through successive iteration loops, which can be easily coded into a short software routine using simple languages, it is possible to obtain the values of the parameters of the equivalent electrical circuit with the desired accuracy. The application of the method allows an accurate estimation of the output current of the PV panel, taking into account of any changing external conditions. This goal is achieved by assuming that R_s, R_{sh}, and I_0 must change with the solar irradiance because a PV cell and an illuminated semiconductor diode have different electrical behaviour and therefore cannot be represented using the same equivalent model.

The comparison with the data issued by manufacturers of two different silicon PV modules has confirmed the reliability and the quality of the new analytical model. Furthermore, the accuracy of the new model was tested by comparison with models proposed by other authors, and a better agreement with the technical data issued in standard conditions was reached using the new model compared to the previously existing models.

Appendix A. Supporting information

Supplementary data associated with this article can be found in the online version at doi:10.1016/j.solmat.2010.04.003.

References

[1] W. Shockle, Electrons and Holes in Semiconductors, Van Nostrand, New York, 1950.
[2] M. Wolf, H. Rauscenbach, Series resistance effects on solar cell measurements, Advanced Energy Conversion 3 (1963) 455–479.
[3] T. Markvart, L. Costañerv, Solar Cells. Materials, Manufacture and Operation, Elsevier, Oxford, 2005.
[4] N. Enebish, D. Agchbayar, S. Dorjkhand, D. Baatar, I. Ylemj, Numerical analysis of solar cell current-voltage characteristics, Solar Energy Materials and Solar Cells 29 (1993) 201–208.
[5] A. Hovinen, Fitting of the solar cell IV-curve to the two diode model, Physica Scripta T54 (1994) 175–176.
[6] C.L. Garrido-Alzar, Algorithm for extraction of solar cell parameters from I–V curve using double exponential model, Renewable Energy 10 (1997) 125–128.
[7] M. Akbaba, M.A.A. Alattawi, A new model for I–V characteristic of solar cell generators and its applications, Solar Energy Materials and Solar Cells 37 (1995) 123–132.
[8] O. Ortiz-Conde, F.J. Garcia Sanchez, J. Muci, New method to extract the model parameters of solar cells from the explicit analytic solutions of their illuminated I–V characteristics, Solar Energy Materials and Solar Cells 90 (2006) 352–361.
[9] W. De Soto, S.A. Klein, W.A. Beckman, Improvement and validation of a model for photovoltaic array performance, Solar energy 80 (2006) 78–88.
[10] T.U. Townsend, A method for estimating the long-term performance of direct-coupled photovoltaic systems, MSc thesis, Mechanical Engineering, University of Wisconsin–Madison, 1989.
[11] M.A. de Blas, J.L. Torres, E. Prieto, A. Garcia, Selecting a suitable model for characterizing photovoltaic devices, Renewable Energy 25 (2002) 371–380.
[12] A.N. Celik, N. Acikgoz, Modelling and experimental verification of the operating current of mono-crystalline photovoltaic modules using four-and five-parameter models, Applied Energy 84 (2007) 1–15.
[13] A. Hadj Arab, F. Chenlo, M. Benghanem, Loss-of-load probability of photovoltaic water pumping systems, Solar Energy 76 (2004) 713–723.